Egypt. J. Chem. **Vol. 66**, No. SI 13 pp. 2191 - 2200 (2023)

Egyptian Journal of Chemistry

http://ejchem.journals.ekb.eg/

Effects of thermophoresis and mixed convection on Carreau fluid flow with gold nanoparticles

Mohamed Y. Abou-zeid and Mahmoud E. Ouaf*

Department of Mathematics, Faculty of Education, Ain Shams University, Heliopolis, Cairo, 11757, Egypt.

.

Abstract

This study examines non-Newtonian nanofluid flow with heat transfer via a non-Darcy porous medium in the presence of effects. Additionally, the effects of the heat source, viscous and Ohmic dissipation, chemical reaction, electromagnetic field, and Biot number are taken into account. The non-linear equations that control the flow can be made simpler by using appropriate similarity transformations. Then, using a shooting and matching approach, the Rung-Kutta-Merson method is utilised to derive numerical solutions for the velocity, temperature, and concentration of nanoparticles as functions of the problem's physical parameters. This analysis could lead to the development of a model that could help in the understanding of the mechanics of physiological fluids. Additionally, the implications of these parameters on these solutions are studied numerically and graphically. It is discovered that as the Biot number rises or falls, both tangential and normal velocities change. While the temperature increases or decreases as the pressure gradient and radiation parameters increase, the concentration of nanoparticles increases or decreases as the Schmidt numbers and magnetic field parameters increase.

Keywords: Carreau nanofluid; heat transfer; thermophoresis effect; mixed convection; electromagnetic field; chemical reaction.

1.Introduction

Mixed convection takes place when the mechanisms of natural convection and forced convection work together to transfer heat. The phenomenon of mixed convection exists in several technical and industrial issues such as electronic devices chilled by fans, nuclear reactors refrigerated during the emergency stop, a heat exchanger placed in low-velocity surroundings, solar collectors, and so on. [1]. Mixed convective flows driven by differences in temperature and concentration at the different surface geometries through a porous medium have been extensively studied in the past and various extensions of the problems have been reported in the literature. The Mixed convection flow of viscoelastic nanofluid by a cylinder with variable thermalconductivity and heat source/sink is studied by Hayat et al. [2]. Pal and Mondal [3] investigated the effects of Soret and Dufour on MHD non-Darcian mixed convection heat and mass transfer over a stretching sheet with a non-uniform heat source/sink. Mixed convection in a vertical micro-annulus between two concentric micro-tubes was examined by Avci and Aydin [4]. It became apparent that the increase in the mixed convection parameter increases the heat transfer.

* Corresponding author should be addressed: mouaf68@gmail.com (Mahmoud E. Ouaf)
Received date 03 May 2023; revised date 01 June 2023; accepted date 11 June 2023
DOI: 10.21608/EJCHEM.2023.208687.7925

Some important studies on the subject can be found in [5–7].

Past two decades, non-Newtonian fluid flow studies were taking up greater attention and importance than Newtonian fluids, as far as their various industrial technical applications [8-14]. Nanofluids are a relatively new class of fluids that consist of a base fluid with nano-sized particles (1–50 nm) suspended within them [15]. Nanoparticles being used in nanofluids are usually made of metals, oxides, carbides, or carbon nanotubes. Nanofluids has numerous applications such as transportation (engine cooling/vehicle thermal management), electronics refrigeration, nuclear systems refrigeration, heat exchanger, chemical process, as well as biological medicine. Non-Newtonian nanofluids are commonly available in several industrial technology applications, for example, the thawing of polymers, biological solutions, paints, tars, asphalt, glues, etc. A notable example of these efforts is found in references [16-18]. The problem of MHD non-Newtonian nanofluid flow with a heat transfer under the effect of chemical reaction and radiation through a porous medium has been discussed by Eldabe et al. [19]. Various authors have explored the properties specific to different non-Newtonian nanofluid flows [20–29].

The main objective of this paper is to extend the work ofEldabe et al. [30] in the case ofmixed convection, non-Darcian effect, and non-Newtonian nanofluid, viscous dissipation effect. Because the partial differential equations of velocity,temperature, and nanoparticle concentration are very highly non-linear, it has been transformed into a non-linear ordinary differential equation using the appropriate similarity transformations. This system of equations is solved numerically by the applying Rung-Kutta-Merson method with a Newton iteration in a shooting and matching technique. This analysis could make it a model that can support understanding the mechanics of physiological flows.

2.Mathematical formulations

Cartesian coordinates (x, y, z) are taken into account, where x is along a direction of fluid flow, y is the normal to x, and z perpendicular plane (x y). The electrically conducting Carreau nanofluid is flowing steadily into a shrinking sheet. The external applied magnetic field, while the electric field.

A constitutive model of Carreau fluid may be written as follows:

$$\tau_{ij} = -\eta_0\left[1+\frac{(n-1)}{2}\Gamma^2\dot{\gamma}^2\right]\dot{\gamma}_{ij}\ , \tag{1}$$

$$\dot{\gamma}_{11}=2\frac{\partial u}{\partial x},\quad \dot{\gamma}_{12}=\dot{\gamma}_{21}=\frac{\partial u}{\partial y}+\frac{\partial v}{\partial x},\quad \dot{\gamma}_{22}=2\frac{\partial v}{\partial y}\ , \tag{2}$$

where $\dot{\gamma}$ is defined as:

$$\dot{\gamma}=\sqrt{\frac{1}{2}\sum_i\sum_j\dot{\gamma}_{ij}\dot{\gamma}_{ij}}=\sqrt{\frac{1}{2}\prod_{\dot{\gamma}}}\ , \tag{3}$$

where $\prod_{\dot{\gamma}}$ is a second invariant of strain-rate tensor $\dot{\gamma}_{ij}$.

The equations of continuity, momentum, energy, and nanoparticles concentration can be written, respectively, as [31-33]:

$$\frac{\partial u}{\partial x}+\frac{\partial v}{\partial y}=0, \tag{4}$$

$$u\frac{\partial u}{\partial x}+v\frac{\partial u}{\partial y}=\frac{-1}{\rho}\frac{\partial p}{\partial x}-\frac{\eta_0}{\rho}\frac{\partial}{\partial y}\left\{\left(1+\frac{n-1}{2}\Gamma^2\left(\frac{\partial u}{\partial y}\right)^2\right)\frac{\partial u}{\partial y}\right\}+ \frac{\sigma}{\rho}(E_0B_0-B_0^2u)+g\beta_T(T-T_\infty)+g\beta_C(C-C_\infty)-\frac{\nu}{k}u+C^*u^2, \tag{5}$$

$$u\frac{\partial T}{\partial x}+v\frac{\partial T}{\partial y}=\frac{K}{\rho c_p}\frac{\partial^2 T}{\partial y^2}- \frac{\eta_0}{\rho c_p}\left\{\left(1+\frac{n-1}{2}\Gamma^2\left(\frac{\partial u}{\partial y}\right)^2\right)\frac{\partial u}{\partial y}\right\}\frac{\partial u}{\partial y}+ \frac{\sigma}{\rho c_p}(uB_0-E_0)^2-\frac{1}{\rho c_p}\frac{\partial q_r}{\partial y}+\frac{Q_0}{\rho c_p}(T-T_\infty)+ D_T\left(\frac{\partial T}{\partial y}\right)^2+D_B\left(\frac{\partial T}{\partial y}\right)\left(\frac{\partial C}{\partial y}\right), \tag{6}$$

$$u\frac{\partial C}{\partial x}+v\frac{\partial C}{\partial y}=D_B\frac{\partial^2 C}{\partial y^2}+\frac{D_T}{T_0}\frac{\partial^2 T}{\partial y^2}-A(C-C_\infty), \tag{7}$$

where the thermal radiation heat flux; $q_r = -\frac{4\sigma^*}{3k_0}\frac{\partial T^4}{\partial y}$.We expect that thedifferences in fluid-phase temperatures in flow areenough small that T^4 can be expressed as the linear function of temperature.

$$T^4 = 4T_\infty^3 T - 3T_\infty^4 \quad (8)$$

Simplifying the foregoing system, we apply the following transformations:

$$f'^2 - ff'' = -\frac{\partial p}{\partial x} - \frac{1}{\mathrm{Re}}(1+\frac{n-1}{2}We\, f''^2)f''' - (M^2 - \frac{1}{Da})f' + M^2 E_1 + G_r\theta + B_r\phi + Fs\, f'^2 \quad (10)$$

$$f\theta' = \frac{1+4R}{3\mathrm{Pr}}\theta'' - \frac{Ec}{\mathrm{Re}}\left(1+\frac{n-1}{2}We^2 f''^2\right)f''^2 + Ec\, M^2(f'+E_1)^2 + Q_0\theta + Nt\,\theta' + Nb\,\theta'\varphi' \quad (11)$$

$$Sc\, f\,\varphi' = \varphi'' + \frac{Nt}{Nb}\theta'' - \delta\varphi^m \quad (12)$$

It should be noted that n=1 leads to a boundary-layer flow of ordinary Newtonian conducting fluid. At the same time when we put $F_s = \frac{\partial p}{\partial x}$ =0, n=1 and Bi→ ∞, this problem was investigated for the same boundary conditions by Eldabe et al. [30].Eqs. (10)-(12) are coupled non-linear ordinary differential equations of order three. For Carreau fluid, as the parameter n tends to zero, the fluid is becoming ordinary Newtonian.

The boundary conditions in the non-dimensional form are:

$$f(0)=0,\quad f'(0)=1,\quad \theta(0)=1+\frac{1}{Bi}\theta'(0),\quad \varphi(0)=1$$
$$f'(\infty)=\theta(\infty)=\varphi(\infty)=0. \quad (13)$$

3.Numerical solutions

NAG Fortran libraries with help of subroutine D02HAF will be used to solve the foregoing system of equations (10-12). Moreover, then, the shooting technique is applied. The present subroutine might be needed to suppose missing initial and terminal conditions. The governing equations(10-12) have been solved by the Rung-Kutta-Merson method of order five. In the present subroutine, we haveused variable step size to control a local truncationerror,but then again, the modified Newton-Raphson method is used to get successive corrections at the estimated boundary values.

The process is repeated iteratively several times before convergence and accuracy have occurred.

4. Discussion

Here, we analysed graphically how the temperature, nanoparticle concentration, and the problem's physical parameters affected the tangential and normal velocities. Moreover, we obtained the numerical values of these physical quantities and tabulated the coefficients of skin-friction and both heat transfer and mass transfer by using Mathematica package Ver.10.1. The standard values of these parameters are taken as follows:

$$n = 2, M = 0.5, \mathrm{Da} = 0.1, \mathrm{E1} = 0.5, \frac{\partial p}{\partial x} = -10,$$

Re=0.5, Fs=0.4,We=0.5,Gr=0.5,Br=0.5,Pr=1,R=1

Ec=3.5,Q0=1,Sc=2.5,Bi=0.5,Nt=3.5,Nb = 2.5,

m = 2, δ = 0.8.

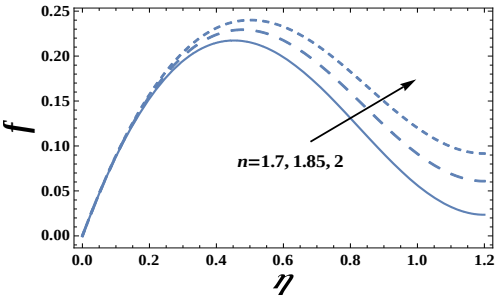

Fig. (1). The variation of f with η, for different values n.

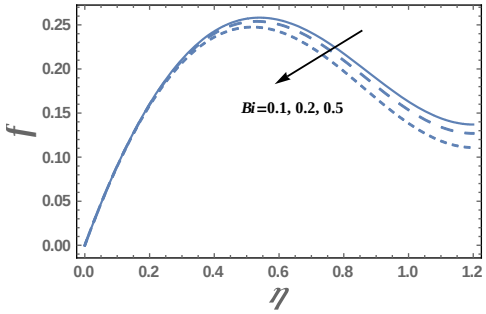

Fig. (2). The variation of f withη, for different values *Bi*.

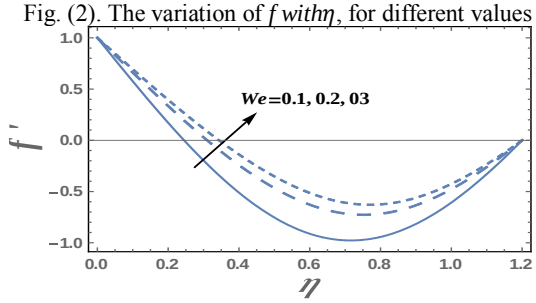

Fig. (3). The variation of f' with η, for different values We.

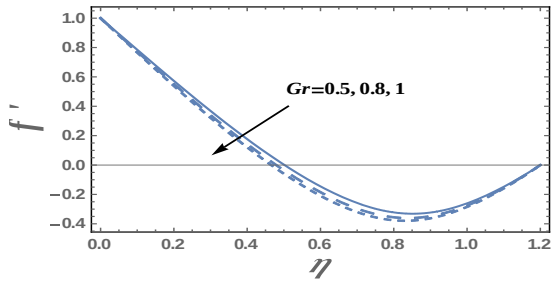

Fig. (4). The variation of f' with η, for different values Gr.

Biot number is a dimensionless quantity that measures the ratio of the reluctance of heat transfer from the inside of the body to the surface of the body. So, a small Biot number reveals low resistance to transport by conduction, and therefore very low-temperature gradients within the body. Figures (1) and (2) display the variations of the normal velocity f versus the dimensionless coordinate η for different values of dimensionless power-law index n and Biot number Bi, respectively. It is noted from these figures that the normal velocity increases with the increase of n, while it decreases as Bi increases. The result in Fig. (2) is due to the above definition of the Biot number. In addition, f increases with η for large values of n, and small values of Bi, till a definite value $\eta = \eta_0$ (represents the maximum value of f) and it decreasesafterward. Furthermore, all curves for different values of both n and Bi are identical near the sheet, namely in the interval η ∈ [0, 0.21], otherwise, the effect of these parameters is clear; this is due to the fact that the shrinking sheet is cold initially. The Weissenberg number is defined by the ratio between elastic and viscous forces. Moreover, it usually measures the relation between the fluid stress relaxation time and a specific process time, i.e. Weissenberg number may help to increase the fluid flow. The variations of the tangential velocity f' with the dimensionless coordinate η for various values of Weissenberg number We and Thermal Grashof number Gr are shown in Figs. (3) and (4), respectively, The graphical results of Figs. (3) and (4), indicate that the tangential velocity increases with an increase in the parameter We, while it decreases by increasing the parameter Gr, Furthermore, It is observed that for small values of We and large values of Gr, the relation between f' and η is a parabola with a down vertex, i.e. f' decreases with η till a definite value η=η0, (represents the minimum value of f') and it increases afterward. This absolute minimum value of f' increases by increasing Gr, while it decreases by increasing We. The above definition of the Weissenberg number explains the result in Fig. (3). Moreover, this result agrees with those presented by [30].

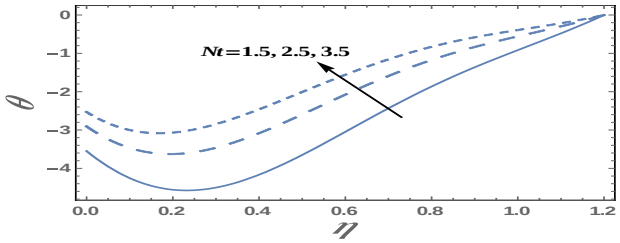

Fig. (5). The variation of $\theta$with η, for different values *Nt*.

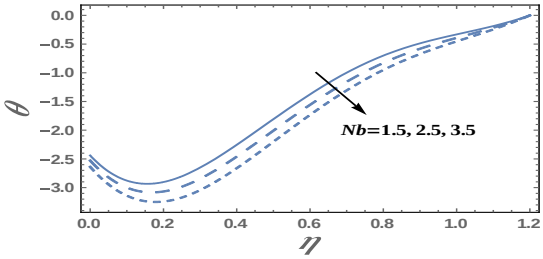

Fig. (6). The variation of $\theta$with η, for different values *Nb*.

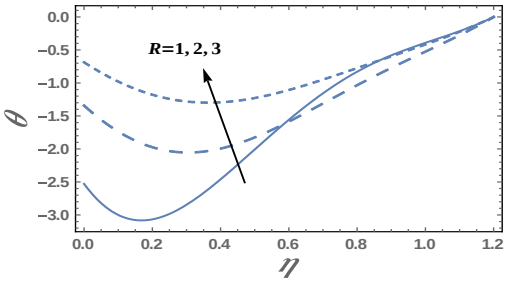

Fig. (7). The variation of $\theta$with η, for different values *R*.

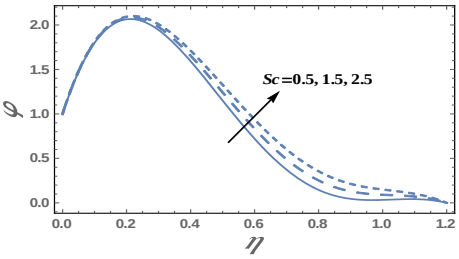

Fig. (8). The variation of $\varphi$with η, for different values *Sc*.

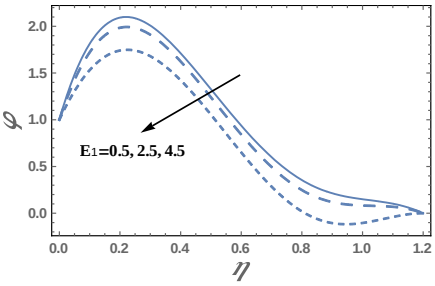

Fig. (9). The variation of $\varphi$with η, for different values E_1.

Figs. (5) and (6) show the behavior of the temperature distribution θ with the dimensionless coordinate η for various values of the thermophoresis parameter Nt and Brownian motion parameter Nb, respectively. It has been seen from these figures that the temperature increases with the increase of Nt, while it decreases as Nb increases. It is also noted that for each value of both Nt and Nb, there exists a minimum value of θ whose absolute value increases by increasing Nb and decreases by increasing Nt, and all minimum values occur at η=0.17. Brownian motion is an inherent flow of particles dangled in a fluid. This random transport agrees with the fact that the temperature decreases with the Brownian motion parameter. So, the result in Fig. (6) agrees with the physical expectation, and is in agreement with those which are presented by [26]. The effect of radiation parameter R on the temperature distribution θ as a function of the dimensionless coordinate η is shown in Fig. (7). It is found that the temperature distribution increases by increasing R in the interval η∈ [0, 0.65]; otherwise it decreases by increasing R. So, the behavior of θ in this interval is an inversed manner of its behavior in the intervalη∈ [0.65, 0.18], except that the curves are quite close to each other in the second interval.

Eq. (12) evaluates how the nanoparticles concentration distribution φ variations with the dimensionless coordinate η. The effects of both Schmidt number Sc and the local electric parameter E1 on the nanoparticles concentration distribution φ are given in figures (8) and (9), respectively. It is found that the nanoparticles concentration increases by increasing Sc, but it decreases by increasing E1. Furthermore, the nanoparticles concentration is always positive, and for large values of Sc and small values of E1, it increases with η till a maximum value of η, after which it decreases.

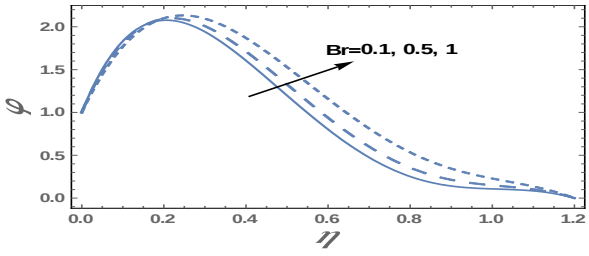

Fig. (10). The variation of $\varphi$with η, for different values *Br*.

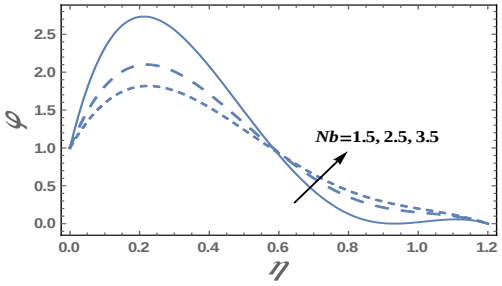

Fig. (11). The variation of $\varphi$with η, for different values *Nb*.

The effect of nanoparticles concentration Grashof number Br on the nanoparticles concentration φ which is a function of η is given in Fig. (10). It is found that the nanoparticles concentration decreases by increasing Nb in the interval η∈ [0, 0.21]; otherwise it increases by increasing η. So, the behavior of φ in the interval η∈ [0, 0.21], is an inversed manner of its behavior in the interval η∈ [0.21, 1.2], and in the first interval, there is a maximum value of φ holds at η =0.2. Figure (11) illustrates the effect of Brownian motion parameter Nb on the nanoparticles concentration φ as a function of η. It is found that the behavior of φ for various values of Nb is in the same manner as the behavior of φ for various values of Br given in Figure (10), except that all curves are very ruffled than to each other than those obtained in Fig. (10).

5. Conclusion

This problem extends the work of Eldabe et al. [30] to include mixed convection, non-Darcian effect, and non-Newtonian nanofluid, viscous dissipation effect. Since the partial differential equations of velocity, temperature, and nanoparticles concentration are very highly non-linear, it has been converted into the non-linear ordinary differential equation by using suitable similarity transformations. This system of equations is solved numerically by applying the Rung-Kutta-Merson method with a Newton iteration in a shooting and matching technique. This analysis can render a model which may support comprehension of the mechanics of physiological flows [34-50]. The obtained results can be outlined as follows.

1) By increasing *n* and *Sc*, *n*, *Br*, and δ both the normal and tangential velocities increase while they decrease as E_1, M, and *Bi* increase. Moreover, they increase or decrease as Da increases.
2) The normal velocity becomes greater with increasing the dimensionless coordinate η and reaches a maximum after which, it decreases, but the tangential velocity has an opposite manner, i.e. it has a minimum value.
3) The temperature distribution increases as Da, δ, Nt, We, and Re increase, while it decreases or increases as Q and Nb increase. Furthermore, it decreases or increases as Bi, Ec, Gr, Pr, R, Br, and Da increase.
4) The temperature becomes lower with increasing the dimensionless coordinate η and reaches a minimum at η=0.18, after which, it increases.
5) The nanoparticles concentration has an opposite behavior with respect to the temperature behavior except that it decreases with the increase of δ, Gr, Br, and We.

Data availability

The datasets generated and/or analyzed during the current study are not publicly available due to [All the required data are only with the corresponding author] but are available from the corresponding author on reasonable request.

Acknowledgment

The authors would like to express their sincere gratitude to the anonymous referee for her useful comments.

Conflict of interest

The authors have declared that this paper has no conflict of interest.

Nomenclature

A Reaction rate constant
B_0 Constant
Bi Biot number
Br Concentration Grashof number
C The nanoparticles concentration
C^* Forchheimer ṡ constant
cp The specific heat at constant pressure
Da Darcy number
D_B Brownian diffusion coefficient
D_T Thermophoretic diffusion coefficient
E_0 Constant
E_1 Local electric parameter
Ec Eckert number
Fs Forchheimer number
p The fluid pressure
Pr Prandtl number
q_r Thermal radiation heat flux
Q_0 Heat source parameter
R Radiation parameter
Re Reynolds number
Sc Schmidt number
T The fluid temperature
u The tangential component of velocity
v The normal component of velocity
We Weissenberg number
x Tangential coordinate
y Normal coordinate

Greek symbols

δ Chemical reaction parameter
η_0 Zero-shear-rate viscosity
Γ time constant
ν Kinematic viscosity
ρ Fluid density
σ The electrical conductivity of the fluid
σ^* Stefan-Boltzmann constant
τ_{ij} the stress tensor components,

References

[1] Srinivasacharya, D. & Reddy, G. S. Soret and Dufour effects on mixed convection from a vertical plate in power-law fluid saturated porous medium. J. Theor. Appl. Mech. 40, 525–542 (2013).
[2] Hayat, T., Waqas, M., Sabir, A. S. & Alsaedi, A. Mixed convection flow of viscoelastic nanofluid by a cylinder with variable thermal conductivity and heat source/sink. Int. J. Numer. Methods Heat Fluid Flow. 26, 214–234 (2016).
[3] Kaladhar, K., Motsa, S. S. & Srinivasacharya, D. Mixed convection flow of couple stress fluid in a vertical channel with radiation and soret effects. J. Appl. Fluid Mech., 9, 43–50 (2016).
[4] Avci, M. & Aydin, O. Mixed convection in a vertical micro-annulus between two concentric micro-tubes. ASME J. Heat Transf. 131, 014502–4 (2009).
[5] Eldabe, N. T. M., Abou-zeid, M. Y., Abosaliem, A. Alana, A. & Hegazy, N. Homotopy perturbation approach for Ohmic dissipation and mixed convection effects on non-Newtonian nanofluid flow between two co-axial tubes with peristalsis. Int. J. of Appl. Electromagn. Mech. 67, 153-163 (2021).
[6] Eldabe, N. T. M., Abou-zeid, M. Y., Elshabouri, S. M. Salama, T. N. & Ismael, A. M. Ohmic and viscous dissipation effects on micropolar non-Newtonian nanofluid 〖Al〗_2 O_3 flow through a non-Darcy porous media. Int. J. of Appl. Electromagn. Mech. 68, 209-221 (2022).
[7] Eldabe, N. T., Abou-zeid, M. Y., Mohamed, M. A. & Maged, M. Peristaltic flow of Herschel Bulkley nanofluid through a non-Darcy porous medium with heat transfer under slip condition, Int. J. of Appl. Electromagn. Mech. 66, 649-668 (2021).
[8] N. Hegazy, N.T. Eldabe, M.Y. Abouzeid, A. Abousaleem, and A. Alana, Influence of both chemical reaction and electro-osmosis on MHD non-Newtonian fluid flow with gold nanoparticles. Egyptian Journal of Chemistry, 66 (2023). 191-201.

[9] Eldabe, N. T., Hassan, M A. & Abou-zeid, M. Y. Wall properties effect on the peristaltic motion of a coupled stress fluid with heat and mass transfer through a porous medium. J. Eng. Mech. 142, 04015102 (2015).
[10] Mahomed, F.M. & Hayat, T. Note on an exact solution for the pipe flow of a third-grade fluid. Acta Mech. 190, 233–236 (2007).
[11] O. S. Ahmed, N. T. Eldabe, M. Y. Abou-zeid, O. H. El-kalaawy and S. M. Moawad, Numerical treatment and global error estimation for thermal electro-osmosis effect on non-Newtonian nanofluid flow with time periodic variations, Sci. Rep. 13 (2023) 14788.
[12] H. A. Sayed and M. Y. Abouzeid, Radially varying viscosity and entropy generation effect on the Newtonian nanofluid flow between two co-axial tubes with peristalsis. Scientific Reports 13 (2023), 11013.
[13] Abu-zeid, M.Y. & Ouaf, M. E. Hall currents effect on squeezing flow of non-Newtonian nanofluid through a porous medium between two parallel plates. Case Stud. Therm. Eng. 28, 10362(2021).
[14] Malik, M.Y., Hussain, A. Nadeem, S. & Hayat, T. Flow of a third-grade fluid between coaxial cylinders with variable viscosity. Z. Naturforsch. A. 64, 588–596 (2009).
[15] Choi, S.U.S. Nanofluids: from vision to reality through research. J. Heat Transfer. 131, 1–9 (2009).
[16] Choi, S.U.S. & Eastman, J.A. Enhancing thermal conductivity of fluids with nanoparticles. in: The proceedings of the ASME International Mechanical Engineering Congress and Exposition. ASME. San Francisco. 66, 99–105 (1995).
[17] Khanafer, K. & Vafai, K. A critical synthesis of thermophysical characteristics of nanofluids. Int. J. Heat Mass Transfer. 54, 4410–4428 (2011).
[18] Wong, K.V. & Leon, O. Applications of nanofluids: current and future. Adv. Mech. Eng. 2010, 1–11 (2010).
[19] Eldabe, N. T. Shaaban, A. Abou-zeid, M.Y. & Ali, H.A. Magnetohydrodynamic non-Newtonian nanofluid flow over a stretching sheet through a non-Darcy porous medium with radiation and chemical reaction. J. Comput. Theor. Nanosci. 12, 5363–5371 (2015).
[20] El-Dabe, N.T., Abou-Zeid, M.Y. & Ahmed, O.S. Motion of a thin film of a fourth-grade nanofluid with heat transfer down a vertical cylinder: Homotopy perturbation method application. J. Adv. Res. Fluid Mech. Therm. Sci. 66, 101-113 (2020).
[21] Abou-zeid, M.Y. Implicit homotopy perturbation method for MHD non-Newtonian nanofluid flow with Cattaneo-Christov heat flux due to parallel rotating disks. J. nanofluids. 8,1648-1653(2019).
[22] Abuiyada, A. Eldabe, N. T., Abouzeid, M. Y. Elshabouri, S. Influence of both Ohmic dissipation and activation energy on peristaltic transport of Jeffery nanofluid through a porous media, CFD Letters 15, Issue 6 (2023) 65-85.
[23] Abuiyada, A. Eldabe, N. T., Abouzeid, M. Y. Elshabouri, S. Influence of both Ohmic dissipation and activation energy on peristaltic transport of Jeffery nanofluid through a porous media, CFD Letters 15, Issue 6 (2023) 65-85.
[24] Eldabe, N.T., Moatimid, G. M., Abouzeid, M.Y., ElShekhipy, A.A. & Abdallah, N.F. A semi-analytical technique for MHD peristalsis of pseudoplastic nanofluid with temperature-dependent viscosity: Application in drug delivery system. Heat Trans. Asian Res. 49, 424-440 (2020).
[25] Eldabe, N.T., Moatimid, G. M., Abouzeid, M.Y., ElShekhipy, A.A. & Abdallah, N.F. Instantaneous thermal-diffusion and diffusion-thermo effects on carreau nanofluid flow over a stretching porous sheet. J. Adv. Res. Fluid Mech. Therm. Sci. 72. 142-157 (2020).
[26] M.El. Ouaf and M. Abou-zeid, Electromagnetic and non-Darcian effects on a micropolar non-Newtonian fluid boundary-layer flow with heat and mass transfer. International Journal of Applied Electromagnetics and Mechanics. **66**, 693-703, (2021).
[27] Eldabe, N. T. M., Moatimid, G. M., Abou-zeid, M. Y., Elshekhipy, A. A. & Abdallah, N. F. Semi-analytical treatment of Hall current effect on peristaltic flow of Jeffery nanofluid. Int. J. Appl. Electromagn. Mech.7, 47-66 (2021).
[28] Ouaf, . M. E., Abouzeid, M. Y. & Younis, Y. M. Entropy generation and chemical reaction effects on MHD non-Newtonian nanofluid flow in a sinusoidal channel. Int.

J. of Appl. Electromagn. Mech. 69, 45-65 (2022).

[29] Eldabe, N. T. M., Abou-zeid, M. Y. Abosaliem, A., Alana, A. & Hegazy, N. Thermal Diffusion and Diffusion Thermo Effects on Magnetohydrodynamics Transport of Non-Newtonian Nanofluid Through a Porous Media Between Two Wavy Co-Axial Tubes. IEEE Trans. Plasma Sci. 50, 1282-1290 (2021).

[30] Ibrahim, M. Abdallah, N. & Abouzeid, M. Activation energy and chemical reaction effects on MHD Bingham nanofluid flow through a non-Darcy porous media. Egypt. J. Chem. 65, 715 – 722(2022).

[31] Eldabe, N. T., Abou-zeid, M. Y., El-Kalaawy, O. H., Moawad, S. M. & Ahmed, O. S. Electromagnetic steady motion of Casson fluid with heat and mass transfer through porous medium past a shrinking surface. Therm. Sci. 25, 257-265 (2021).

[32] Ismael, A.M., Eldabe, N.T.M., Abouzeid, M.Y., & Elshabouri, S.M. Thermal micropolar couple stresses effects on peristaltic flow of biviscosity nanofluid through a porous medium. Scientific Reports 12, 16180 (2022).

[33] Abouzeid, M.Y. Chemical reaction and non-Darcian effects on MHD generalized Newtonian nanofluid motion. Egy. J. Chem. 65, 647-655 (2022).

[34] Abouzeid, M.Y., & Ibrahim, M. G. Influence of variable velocity slip condition and activation energy on MHD peristaltic flow of Prandtl nanofluid through a non-uniform channel. Scientific Reports 12, 18747 (2022).

[35] Eldabe, N. T., Elshabouri, S., Elarabawy, H., Abouzeid, M. Y. & Abuiyada, A. J. Wall properties and Joule heating effects on MHD peristaltic transport of Bingham non-Newtonian nanofluid. Int. J. of Appl. Electromagn. Mech. 69, 87–106 (2022).

[36] Ismael, A., Eldabe, N., Abouzeid, M. & Elshabouri, S. Activation energy and chemical reaction effects on MHD Bingham nanofluid flow through a non-Darcy porous media. Egypt. J. Chem. 65, 715–722 (2022).

[37] Mansour, H. M. & Abouzeid, M. Y. Heat and mass transfer effect on non-Newtonian fluid flow in a non-uniform vertical tube with peristalsis. J. Adv. Res. Fluid Mech. Therm. Sci., 61, 44-64 (2019).

[38] M. G. brahim and M. Y. Abouzeid, Computational simulation for MHD peristaltic transport of Jeffrey fluid with density-dependent parameters. Scientific Reports 13 (2023), 9191.

[39] Mohamed, Y. M., Eldabe, N. T., Abou-zeid, M. Y., Mostapha, D. R.& ouaf, M. E., Impacts of chemical reaction and electric field with Cattaneo - Christov theories on peristaltic transport of a hyperbolic micropolar nanofluid, Egyptian Journal of Chemistry, 66 (7) (2023) 63 – 85.

[40] Eldabe, N. T., Abouzeid, M. Y. Mohamed, M. A. A., Abd-Elmoneim, M. M. Peristaltic mixed convection slip flow of a Bingham nanofluid through a non-darcy porous medium in an inclined non-uniform duct with viscous dissipation and radiation. J. of Appl. Nonlinear Dyn. 12, 231-243 (2023).

[41] Mohamed, Y. M., Eldabe, N. T., Abou-zeid, M. Y., Ouaf, M. E.& Mostapha, D. R., Chemical reaction and thermal radiation via Cattaneo-Christov double diffusion (ccdd) effects on squeezing non-Netonian nanofluid flow between two - parallel plates, Egyptian Journal of Chemistry, 66 (3) (2023) 209 – 231.

[42] Abdelmoneim, M., Eldabe, N.T., Abouzeid, M.Y., Ouaf, M.E.: Both modified Darcy's law and couple stresses effects on electro-osmotic flow of non-Newtonian nanofluid with peristalsis. Int. J. Appl. Electromagn. Mech. 72(3), 253–277 (2023).

[43] M. Ouaf, M. Abouzeid, and M.G.Ibrahim, Effects of both variable electrical conductivity and microstructural/multiple slips on MHD flow of micropolar nanofluid. Egyptian Journal of Chemistry, 66 (2023). 449-456.

[44] N.T. Eldabe, M.Y. Abou-zeid and H. A. Shawky, MHD peristaltic transport of Bingham blood fluid with heat and mass transfer through a non-uniform channel, J. Adv. Res. Fluid Mech. *Thermal Science*, **77** (2021), 145–159.

[45] Abuiyada, A. J., Eldabe, N. T., Abouzeid, M. Y., Elshabouri, S., Effects of thermal diffusion and diffusion thermo on a chemically reacting MHD peristaltic transport of Bingham plastic nanofluid. Journal of Advanced Research in Fluid Mechanics and Thermal Sciences 98 (2) (2022), 24-43.

[46] Mohamed, Y.M., El-Dabe, N.T., Abou-zeid, M.Y., Oauf, M.E., Mostapha, D.R., Effects of thermal diffusion and diffusion thermo on a chemically reacting MHD peristaltic transport of Bingham plastic nanofluid. Journal of Advanced Research in Fluid Mechanics and Thermal Sciences 98 (1) (2022), 1-17.

[47] N. T. M. Eldabe, M. Y. Abouzeid, and H.A. Ali, Effect of heat and mass transfer on Casson fluid flow between two co-axial tubes with peristalsis, J. Adv. Res. Fluid Mech. Therm. Sci. 76(1) 2020 54-75.

[48] Shaaban, A.A., Abou-Zeid, M.Y. Effects of heat and mass transfer on MHD peristaltic flow of a non-newtonian fluid through a porous medium between two coaxial cylinders, Mathematical Problems in Engineering, 819683 (2013).

[49] N. T. Eldabe, M.Y. Abou-zeid, M. E. Ouaf, D. R. Mustafa, and Y. M. Mohammed, Cattaneo – Christov heat flux effect on MHD peristaltic transport of Bingham nanofluid through a non – Darcy porous medium. International Journal of Applied Electromagnetics and Mechanics, **68**, 59-84, (2022).

[50] N.T.M. Eldabe, R.R. Rizkallah, M.Y. Abou-zeid, and V.M. Ayad, Effect of induced magnetic field on non-Newtonian nanofluid Al2O3 motion through boundary-layer with gyrotactic microorganisms. Thermal Science, **26**, 411 – 422, (2022).